Carbon Nanocoils

High-Performance Direct Methanol Fuel Cell Electrodes using Solid-Phase-Synthesized Carbon Nanocoils**

Taeghwan Hyeon, Sangjin Han, Yung-Eun Sung, Kyung-Won Park, and Young-Woon Kim*

Dedicated to Professor Ki-Jun Lee on the occasion of his retirement

Since the discovery of carbon nanotubes by Iijima in 1991,[1] nanostructured carbon materials[2] have attracted tremendous attention for their possible applications in electron field emitters, catalytic supports, nanocomposites, quantum electronic devices, and electrode materials.[3] Herein we report on

[*] Prof. Dr. T. Hyeon, S. Han
National Creative Research Initiative Center for Oxide Nanocrystalline Materials and
School of Chemical Engineering
Seoul National University
Seoul 151-744 (Korea)
Fax: (+82) 2-886-8457
E-mail: thyeon@plaza.snu.ac.kr
Prof. Dr. Y.-E. Sung, K.-W. Park
Department of Materials Science & Engineering and
Research Center for Energy Conversion and Storage
Kwangju Institute of Science & Technology
Kwangju 500-712 (Korea)
Prof. Dr. Y.-W. Kim
School of Materials Science and Engineering
Seoul National University, Seoul 151-744 (Korea)

[**] T.H. would like to thank the National Creative Research Initiative Program of the Korean Ministry of Science and Technology for financial support. Y.E.S. acknowledges support by the KOSEF through the Research Center for Energy Conversion and Storage.

Supporting information for this article is available on the WWW under http://www.angewandte.org or from the author.

  DOI: 10.1002/ange.200250856

the synthesis of carbon nanocoils composed of nanometer-thick graphitic fibers by the catalytic graphitization of a resorcinol–formaldehyde gel. The carbon nanocoils were successfully applied as electrode materials for direct methanol fuel cells. Many forms of nanostructured carbon materials including carbon nanotubes, graphitic carbon nanofibers (GCNFs), and carbon onions were produced using various gas-phase reactions.[4] Arc discharge, laser evaporation, and thermal chemical vapor deposition are the typical techniques used to produce the materials.[5] However, these synthetic methods have limitations in terms of large-scale and economical production because of their harsh synthetic conditions and low production yields. Although several groups have reported the solid-phase synthesis of nanostructured carbon materials,[6] the synthetic processes used cannot be applied for economical and large-scale production because of the long reaction time or a complicated synthetic procedure.

Carbon is a critical material in low-temperature fuel cells,[7] such as polymer–electrolyte membrane fuel cells. No other material has the essential combination of electronic conductivity, corrosion resistance, surface properties, and the low cost required for the commercialization of fuel cells.[7] In recent years, direct methanol fuel cells (DMFCs) have been intensely studied because of their numerous advantages, which include high energy density, the ease of handling a liquid, low operating temperatures, and their possible applications to micro fuel cells.[8] The performance and long-term stability of low-temperature fuel cells, such as DMFCs, which even operate at room temperature, are known to be strongly dependent on carbon supports as well as catalytically active species.[3e,9] Accordingly, for the best DMFC performance, it is essential to develop a good carbon material for the catalyst support.

We synthesized carbon nanocoils by simply heat-treating composites composed of a carbon precursor, silica, and a transition-metal salt. Resorcinol–formaldehyde (RF) gel was chosen as carbon precursor. A mixture of cobalt and nickel salts was used as the catalyst precursor in the synthesis. A silica sol was added to the reaction mixture to obtain carbon materials with a high specific surface area, and to achieve a good dispersion of the transition-metal nanoparticles, which catalyze the formation of the graphitic carbon nanostructure. We and other research groups have synthesized many different nanoporous carbon materials with amorphous frameworks using nanostructured silica materials as templates.[10] In a typical synthesis, an aqueous reaction mixture, with an H_2O/cobalt salt/nickel salt/resorcinol/formaldehyde/silica molar ratio of 100:0.4:0.4:1:2:0.6, was prepared by mixing the constituent materials in 100 mL of deionized water. The resulting reaction mixture was cured at 85 °C for 3 h in a closed glass vial. For the carbonization, the composite was heated under a nitrogen atmosphere at 900 °C for 3 h. The resulting composite was then stirred in 3 M NaOH solution for 3 h to remove silica particles, and was refluxed in 2.5 M HNO_3 solution for 1 h to remove metal particles, which resulted in the formation of carbon nanocoils (CNCs). Inductively coupled plasma (ICP) analysis revealed that the transition metals were successfully removed by the acid treatment. The current synthetic procedure employs the direct catalytic graphitization of a carbon precursor (RF gel) without the prior synthesis of metal particles, which has been often required in the conventional synthesis of nanostructured carbons.

The XRD pattern of the CNCs (Figure 1) shows that these carbon materials are highly graphitized with a (002) plane *d* spacing of 3.43 Å and clearly observed (100) and (004)

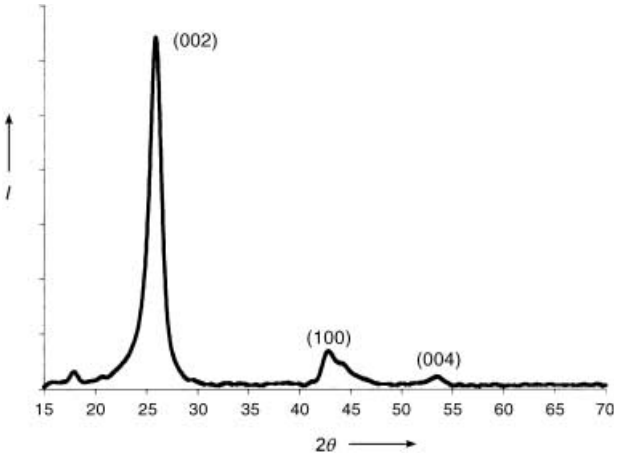

Figure 1. X-ray diffraction (XRD) pattern of carbon nanocoils (CNCs).

peaks. The crystallite size of individual nanocoils measured perpendicular to the basal plane (L_c) using the Debye–Scherrer formula[7] was calculated to be 5.5 nm. Raman spectroscopic data (see Figure S1 in the Supporting Information) showed a characteristic G-band peak at 1576 cm^{-1} and a D-band peak at 1345 cm^{-1}. These XRD and Raman spectroscopic results reveal that the carbon nanocoil possesses a graphitic character that is comparable to multiwall carbon nanotubes. The carbon nanocoils exhibited a high surface area of 318 $m^2 g^{-1}$. The SEM image reveals that the carbon materials consisted of particles of approximately 100 nm diameter (Figure 2a). The TEM image (Figure 2b) shows that each individual particle is composed of 5–10 nm thick coils, which corresponds well with the L_c value of 5.5 nm calculated from the XRD data. The HRTEM image (Figure 2c) of a single nanocoil exhibits well-aligned graphitic layers, which confirm the XRD and Raman spectroscopic results. When the quantity of metal salts used was decreased to 60 wt.% of the amount used for CNC synthesis, a carbon material with an increased surface area of 451 $m^2 g^{-1}$ and a less graphitic structure (as characterized by XRD and Raman spectroscopy) was obtained.

It is well known that it is extremely difficult to synthesize carbon materials with both high surface area and good crystallinity. Consequently, in terms of the design and application for a support in fuel cells, CNCs, which possess high surface area, well-defined porosity, and good crystallinity, are considered to be a very attractive choice. The electrochemical properties of the carbon nanocoils were compared with those of Vulcan XC-72 carbon, which is the most widely used support material for direct methanol fuel cell electrodes. Vulcan XC-72 carbon is amorphous and

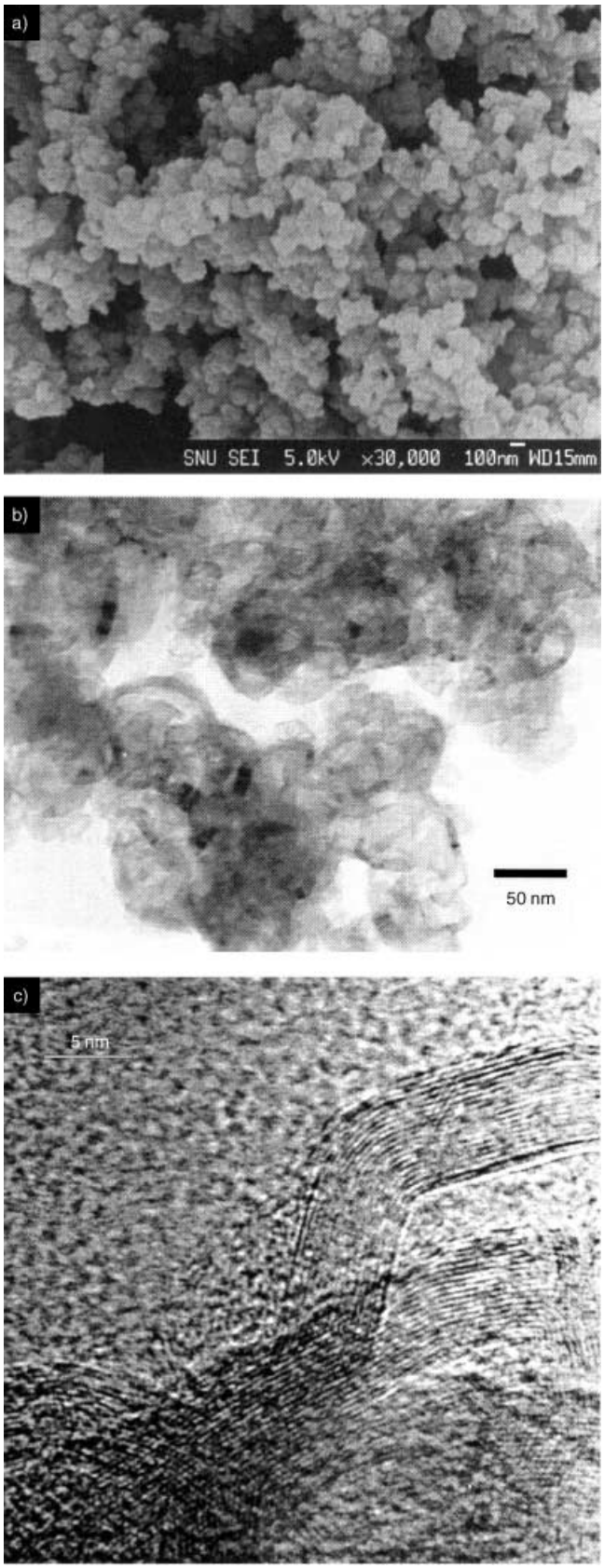

Figure 2. Electron microscope images of carbon nanocoils: a) Field emission scanning electron microscope (FE-SEM) image; b) transmission electron microscope (TEM) image, and c) high-resolution transmission electron microscope (HRTEM) image.

possesses a specific surface area of 212 $m^2 g^{-1}$. The electrochemical stability and capacitance of CNC and Vulcan XC-72 carbons are compared (Figure S2 in the Supporting Information). The catalyst supported on CNC shows excellent electrochemical stability over the potential range of the methanol oxidation process. In addition, it also shows a capacitance over ten times higher than that of Vulcan XC-72 (33.4 versus 2.8 $F g^{-1}$; see the cyclovoltammogram in Figure S2 of the Supporting Information). The TEM image of the supported catalysts (Figure S3 in the Supporting Information) shows the highly dispersed Pt/Ru (1:1) alloy catalyst (60 wt %) on CNC with an average particle size of 2.3 nm, which is in good agreement with the value calculated using Vegard's law and the Debye–Scherrer equation from the XRD pattern (Figure S4 in the Supporting Information). A high catalyst loading of 60 wt % was applied, because the high loading of Pt-based alloy catalysts (especially Pt/Ru) is essential for the anode in DMFCs. The XRD and TEM results showed that the average particle size of Pt/Ru (1:1) alloy nanoparticles supported on Vulcan XC-72, CNCs, and the commercial E-TEK catalyst is similar (≈ 2.3 nm). Further, the active surface area of the supported catalysts was measured using CO chemisorption (Pt-CO) and hydrogen adsorption/desorption (Pt-H) methods. The active surface area is highest for the CNC-supported catalyst and lowest for commercial E-TEK, which means that the catalyst is better dispersed on CNC, compared to other supports (see Table S1 in the Supporting Information). The uniform distribution of the catalyst, along with a small particle size, which are key factors for the stable and efficient operation of a DMFC, seems to result from the good characteristics of CNCs, such as high crystallinity and larger surface area.[11] In order to evaluate the electrocatalytic activity of carbon-supported catalysts, the methanol oxidative current of the catalysts was measured using a fundamental electrochemical system. As shown in Figure 3, the CNC-supported catalyst exhibited a substantially higher specific oxidation current of 80 $A g^{-1}$ at

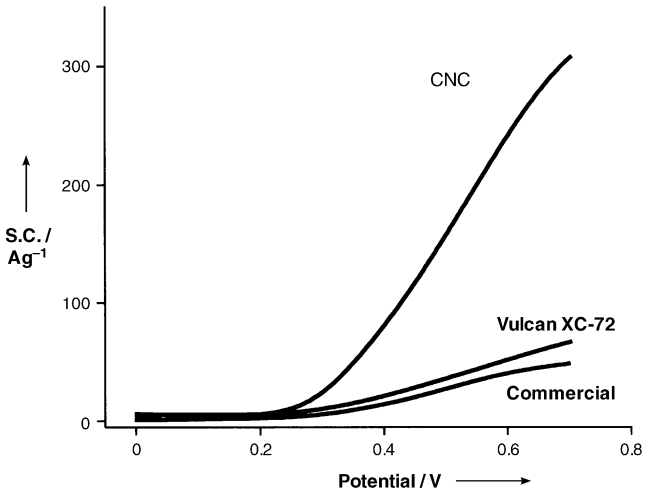

Figure 3. Specific methanol electrooxidation current (S.C.) with respect to applied potentials (versus NHE) of a Pt/Ru (1:1) alloy catalyst (60 wt %) supported on carbon nanocoils (CNC), Vulcan XC-72, and a commercial supported catalyst at 25 °C.

0.4 V (versus a normal hydrogen electrode (NHE)) near the kinetically controlled potential in the methanol reaction, compared to 20 $A g^{-1}$ for the Vulcan XC-72 supported catalyst and 14 $A g^{-1}$ for the E-TEK supported catalyst; the reported methanol oxidation current of Vulcan XC-72 supported Pt/Ru catalysts was also $\approx 20 A g^{-1}$ at the same potential.[12] The remarkably higher oxidation current of the CNC-supported catalyst is directly related to the high surface area and the superior dispersion of the catalyst on CNC. It is also evident that the high electrical conductivity of graphitic CNC, compared with the amorphous Vulcan XC-72, can deliver a significantly higher methanol oxidation current. When the catalytic activity at the same active site of the catalyst is considered, the CNC-supported catalyst is still superior to other catalysts for methanol oxidation. For example, at 0.4 V, the CNC-supported catalyst shows a higher methanol oxidation current density of 46 $\mu A cm^{-2}$, compared to 14 and 12 $\mu A cm^{-2}$ for Vulcan XC-72 and the commercial E-TEK catalyst, respectively. This implies that the enhanced methanol oxidation of the CNC-supported catalyst results not only from the higher active surface area but also from the superior characteristics of the support itself. In addition, the methanol oxidation current of the CNC-supported Pt/Ru catalyst shows a considerably lower onset potential and higher oxidative current than the Vulcan XC-72 supported catalyst. Theoretically, methanol oxidation may proceed at 0.04 V (versus NHE) according to the equation $CH_3OH + H_2O \rightarrow CO_2 + 6H^+ + 6e^-$. Therefore, the lower onset potential demonstrates clear evidence of its superior electrocatalytic activity for methanol electrooxidation.[13] It is believed that both supported Pt/Ru catalysts should start to oxidize methanol at the same potential. However, as indicated in Figure 3, the on-set potentials for CNC- and Vulcan XC-72 supported catalysts are 0.20 and 0.26 V versus NHE, respectively.

The final requirement for carbon-supported catalysts is their successful application to the electrodes in actual DMFC systems consisting of polymer membranes and electrodes. It is well known that at low temperature, the catalysts (including the supports) have a dominating effect on the performance of fuel cells, and comparisons of DMFC performance at relatively low temperatures are the most practical and powerful ways of evaluating the activity of catalysts. Figure 4 shows the polarization curves of a direct methanol fuel cell at 30 and 60 °C using carbon-supported catalysts as the anode. At 0.6 V (Figure 4a), an activation polarization regime dominates the activity of the catalyst; the current density (20 $mA cm^{-2}$) of the CNC-supported catalyst is four and twenty times higher than those of Vulcan XC-72 supported catalyst (5 $mA cm^{-2}$) and the commercial carbon-supported Pt/Ru catalyst (1 $mA cm^{-2}$), respectively. In addition, the CNC-supported catalyst produces a higher maximum power density at 30 °C, which is 170 and 230 % higher than that of the Vulcan XC-72 supported catalyst and the commercial catalyst, respectively. At 60 °C (Figure 4b), the maximum power density of the CNC-supported catalyst is 146 and 180 % higher than the Vulcan XC-72 supported catalyst and the commercial catalyst, respectively. Such an improved activity indicates that the use of CNCs can lead to a substantial reduction of catalyst quantities in the fuel cell. The excellent performance of CNCs is due mainly to the superior electrocatalytic activity for methanol oxidation of the supported catalyst. In addition, the low electrical resistance for current collection and the unique pore characteristics of the support, which favor the diffusion of methanol fuel and the removal of the by-product CO_2 gas, are responsible for the improved fuel cell performance. Detailed studies on the origins of the excellent performance of the CNC-supported catalysts will be reported in the future. From combining the results of the electrochemical cell and the practical unit cell, we conclude that carbon nanocoils (CNCs) are an excellent support for the electrodes of direct methanol fuel cells. Further, in the performance of fuel cells, the durability of the electrode is significant for long-term applications. The CNC maintained stable catalytic activity by measuring power density versus time for up to 100 hr in a DMFC unit cell. Accordingly, it is believed that CNC is a highly promising electrode for long-term fuel cells. However, since the issue of durability and stability of the fuel cell electrode is very important, a more profound study of these characteristics is underway.

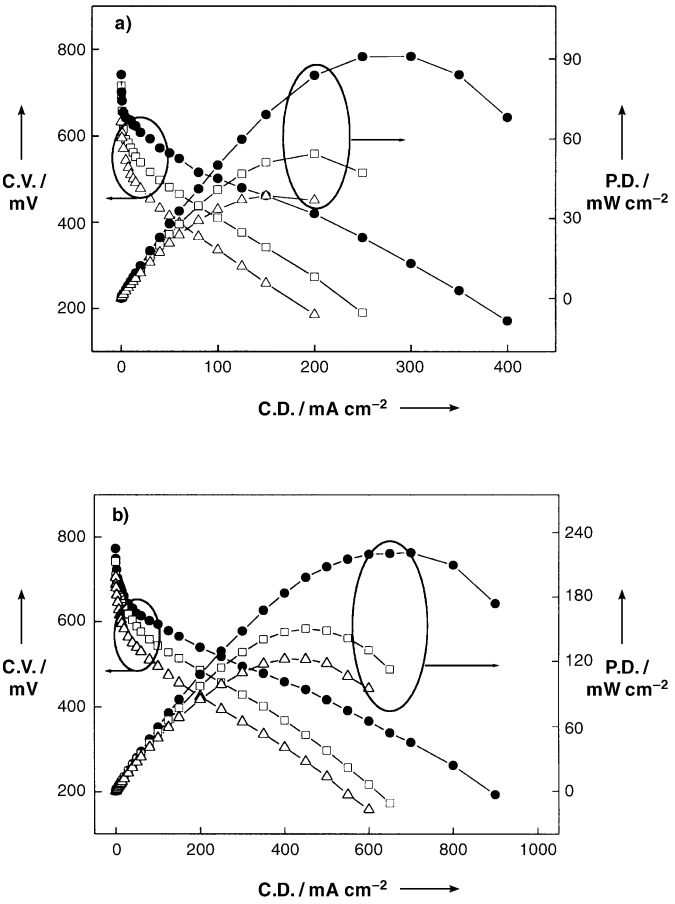

Figure 4. Polarization curves for a direct methanol fuel cell using a Pt/Ru (1:1) alloy catalyst (60 wt %) supported on carbon nanocoils (CNC; ●), Vulcan XC-72 (□), and a commercial supported catalyst (△): a) 30 °C; b) 60 °C. C.V., C.D., and P.D. stand for cell voltage, current density, and power density, respectively.

Experimental Section

Carbon-supported catalysts were synthesized at room temperature by a conventional reduction method using $H_2PtCl_6 \cdot 6H_2O$, $RuCl_3 \cdot x H_2O$, (both Aldrich) and $NaBH_4$ as the reductant.[14]

Electrochemical measurements were conducted using a three-electrode cell at 25 °C. Pt gauze and Ag/AgCl (in saturated KCl) were used as the counter and reference electrodes, respectively. The carbon working electrode (6 mm in diameter) was polished with 1, 0.3, and 0.05 μm Al_2O_3 paste and washed ultrasonically in Millipore water (18 MΩ cm). The commercial carbon-supported Pt/Ru (60 wt %) catalyst was purchased from E-Tek Inc. The catalyst ink consisting of catalyst, Nafion ionomer (in water), and 2-propanol was dropped onto the working electrode, and dried at 70 °C in a vacuum oven. Solutions of 0.5 M H_2SO_4 and 2.0 M CH_3OH in 0.5 M H_2SO_4 were stirred constantly and purged with nitrogen gas. All chemicals used were of analytical grade. Electrochemical experiments were performed using an AUTOLAB by Eco Chemie. In order to compare the catalytic activity of the supported catalysts for methanol oxidation, voltammetry was performed in the potential range 0–0.7 V versus NHE.

For a membrane electrode assembly (MEA) of DMFC, an anode (supported catalysts) prepared from Pt/Ru (2 mg per cm^2) and a cathode prepared from Pt black (5 mg per cm^2; Johnson Matthey Co.) was formed on teflon-coated carbon paper (TGPH-090) substrates using catalyst inks containing the appropriate weight percentage of Nafion ionomer solution (Aldrich). The MEA for unit cell tests was fabricated by pressing as-prepared cathode and anode layers onto both sides of a pretreated Nafion 117 electrolyte membrane at 110 °C and 800 psi for 3 min. Cell performance was evaluated in a DMFC unit cell with a 2 cm^2 cross-sectional area, and measured with a potentiometer (WMPG-3000), which recorded the cell under a constant current. Both fuel and oxidant flow paths were machined into graphite block end-plates, which also served as current collectors. A 2 M methanol solution with a flow rate of 1 $cm^{-3}\,min^{-1}$ was supplied by a Masterflex liquid micropump, and a dry O_2 flow was regulated at 500 $cm^{-3}\,min^{-1}$ using a flowmeter.

Received: December 27, 2002
Revised: July 14, 2003 [Z50856]

Keywords: carbon · fuel cells · nanomaterials · solid-phase synthesis · supported catalysts

[1] S. Iijima, *Nature* **1991**, *354*, 56–58.
[2] a) S. Subramoney, *Adv. Mater.* **1998**, *10*, 1157–1171; b) *Supercarbon* (Eds.: S. Yoshimura, R. P. H. Chang), Springer, Berlin, **1998**; c) *Science and Application of Nanotubes* (Eds.: D. Tománek, R. J. Enbody), Kluwer, Dordrecht, **2000**.
[3] a) W. A. Heer, A. Chatelan, D. Ugarte, *Science* **1995**, *270*, 1179–1180; b) J. M. Planeix, N. Coustel, B. Coq, V. Brotons, P. S. Kumbhar, R. Dutarte, P. Geneste, P. Bernier, P. M. Ajayan, *J. Am. Chem. Soc.* **1994**, *116*, 7935–7936; c) X. Gong, J. Liu, S. Baskaran, R. D. Voise, J. S. Young, *Chem. Mater.* **2000**, *12*, 1049–1052; d) J. Hu, M. Ouyang, P. Yang, C. M. Lieber, *Nature* **1999**, *399*, 48–51; e) C. A. Bessel, K. Laubernds, N. M. Rodriguez, R. T. K. Baker, *J. Phys. Chem.* B **2001**, *105*, 1115–1118.
[4] a) F. T. Edelmann, *Angew. Chem.* **1999**, *111*, 1473–1480; *Angew. Chem. Int. Ed.* **1999**, *38*, 1381–1387; b) N. M. Rodriguesz, *J. Mater. Res.* **1993**, *8*, 3233–3250; c) D. Ugarte, *Nature* **1992**, *359*, 707–709.
[5] a) T. W. Ebbesen, P. M. Ajayan, *Nature* **1992**, *358*, 220–221; b) A. Thess, R. Lee, P. Nikolaev, H. Dai, P. Petit, J. Robert, C. Xu, Y. H. Lee, S. G. Kim, A. G. Rinzler, D. T. Colbert, G. E. Scuseria, D. Tomanek, J. E. Fischer, R. E. Smalley, *Science* **1996**, *273*, 483–487; c) S. Fan, M. C. Chapline, N. R. Frankin, T. W. Tombler, A. M. Cassell, H. Dai, *Science* **1999**, *283*, 512–514.
[6] a) W. Cho, E. Hanada, Y. Kondo, K. Takayanagi, *Appl. Phys. Lett.* **1996**, *69*, 278–279; b) N. A. Kiselev, J. Sloan, D. N. Zakharov, E. F. Kukovitskii, J. L. Hutchison, J. Hammer, A. S. Kotosonov, *Carbon* **1998**, *36*, 1149–1157; c) F. J. Maladonado-Hodar, C. Moreno-Castilla, J. Rivera-Utrilla, Y. Hanazawa, Y. Yamada, *Langmuir* **2000**, *16*, 4367–4373.
[7] a) K. Kinoshita, *Carbon, Electrochemical and Physicochemical Properties*, Wiley, New York, **1998**; b) *Carbon Materials for Advanced Technologies* (Ed.: T. D. Burchell), Pergamon, New York, **1999**; *Sciences of Carbon Materials* (Eds.: H. Marsh, F. Rodriguez-Reinoso), Publicaciones de la Universidad de Alicante, Alicante, Spain, **1997**.
[8] a) E. Reddington, A. Sapienza, B. Gurau, R. Viswanathan, S. Sarangapani, E. S. Smotkin, T. E. Mallouk, *Science* **1998**, *280*, 1735–1737; b) B. Gurau, R. Viswanathan, R. Liu, T. J. Lafrenz, K. L. Ley, E. S. Smotkin, E. Reddington, A. Sapienza, B. C. Chan, T. E. Mallouk, S. Sarangpani, *J. Phys. Chem.* B **1998**, *102*, 9997–10003; c) K.-W. Park, K.-S. Ahn, J.-H. Choi, Y.-C. Nah, Y.-M. Kim, Y.-E. Sung, *Appl. Phys. Lett.* **2002**, *81*, 907–909.
[9] E. S. Steigerwalt, G. A. Deluga, D. E. Cliffel, C. M. Lukehart, *J. Phys. Chem. B.* **2001**, *105*, 8097–8101.
[10] a) J. Lee, S. Yoon, S. M. Oh, C. -H. Shin, T. Hyeon, *Adv. Mater.* **2000**, *12*, 359–362; b) S. Han, K. Sohn, T. Hyeon, *Chem. Mater.* **2000**, *12*, 3337–3341; c) J. Lee, S. Yoon, T. Hyeon, S. M. Oh, K. B. Kim, *Chem. Commun.* **1999**, 2177–2178; d) J. Lee, K. Sohn, T. Hyeon, *J. Am. Chem. Soc.* **2001**, *123*, 5146–5147; e) S. B. Yoon, K. Sohn, J. Y. Kim, C. H. Shin, J. S. Yu, T. Hyeon, *Adv. Mater.* **2002**, *14*, 19–21; f) S. Yoon, J. Lee, T. Hyeon, S. M. Oh, *J. Electrochem. Soc.* **2000**, *147*, 2507–2512; g) S. H. Joo, S. J. Choi, I. Oh, J. Kwak, Z. Liu, O. Terasaki, R. Ryoo, *Nature* **2001**, *412*, 169–172; h) S. Jun, S. H. Joo, R. Ryoo, M. Kruk, M. Jaroniec, Z. Liu, T. Ohsuna, O. Terasaki, *J. Am. Chem. Soc.* **2000**, *122*, 10712–10713; i) R. Ryoo; S. H. Joo, S. Jun, *J. Phys. Chem. B* **1999**, *103*, 7743–7746; j) J. S. Lee, S. H. Joo, R. Ryoo, *J. Am. Chem. Soc.* **2002**, *124*, 1156–1157; k) T. Kyotani, T. Nagai, S. Inoue, A. Tomita, *Chem. Mater.* **1997**, *9*, 609–615; l) Z. Ma, T. Kyotani, A. Tomita, *Chem. Commun.* **2000**, 2365–2366; m) D. Kawashima, T. Aihara, Y. Kobayashi, T. Kyotani, A. Tomita, *Chem. Mater.* **2000**, *12*, 3397–3401; n) Z. Li, M. Jaroniec, *J. Am. Chem. Soc.* **2001**, *123*, 9208–9209.
[11] A. Guerro-Ruiz, P. Badenes, I. Rodriguez-Ramos, *Appl. Catal. A* **1998**, *173*, 313–321.
[12] a) T. J. Schmidt, H. A. Gasteiger, R. J. Behm, *Electrochem. Commun.* **1999**, *1*, 1–4; b) A. Hamnett, S. A. Weeks, B. J. Kennedy, G. Troughton, P. A. Christensen, *Ber. Bunsen-Ges.* **1990**, *94*, 1014–1020.
[13] K.-W. Park, J.-H. Choi, B.-K. Kwon, S.-A. Lee, Y.-E. Sung, H.-Y. Ha, S.-A. Hong, H. Kim, A. Wieckowski, *J. Phys. Chem. B* **2002**, *106*, 1869–1877.
[14] *Modern Aspect of Electrochemisty, Vol. 12* (Eds.: K. Kinoshita, P. Stonehart), Plenum Press, New York, **1996**.

